Multiaxial Deformations of End-linked Poly(dimethylsiloxane) Networks. 2. Experimental Tests of Molecular Entanglement Models of Rubber Elasticity

Kenji Urayama,* Takanobu Kawamura, and Shinzo Kohjiya

Institute for Chemical Research, Kyoto University, Uji, Kyoto-fu 611-0011, Japan

Received December 20, 2000; Revised Manuscript Received July 23, 2001

ABSTRACT: Five molecular models of rubber elasticity which employ different treatments of entanglement effects (the Kloczkowski−Mark−Erman diffused-constraint model, the Edwards−Vilgis (E−V) slip−link model, the tube models of Gaylord−Douglas (G−D), Kaliske−Heinrich, Rubinstein−Panyukov versions) are assessed using biaxial deformation data for an entanglement-dominated network of end-linked poly(dimethylsiloxane) (PDMS) in which trapped entanglements are dominant in number relative to chemical cross-links. The theoretical stress−strain relations were calculated from the elastic free energy (W) of each model. Using the reduced stress (the nominal stress divided by equilibrium modulus G_o), the strain-dependent predictions of each model were tested from two different viewpoints, i.e., the dependence of the reduced stresses on the principal ratio and the I_i dependence of $(\partial W/\partial I_j)/G_o$ ($i,j = 1,2$), where I_1 and I_2 are the first and second invariants of deformation tensor (the Rivlin−Saunders method). The diffused-constraint model is relatively successful in reproducing the reduced stress−strain data over a wide range of deformations, but the model definitely underestimates the magnitude of G_o because it does not consider trapped entanglements as additional cross-links contributing to G_o, in contrast to the tube models and the slip−link models. The G−D tube model is more successful in reproducing the experimental data relative to the other two versions of the tube model, but the G−D model obviously underestimates the stresses at large deformations. Among the five molecular theories tested here, the E−V slip−link model shows the most successful reproducibility over large portions of the experimental results. The agreements in reduced stress−strain relations are satisfactory over the entire deformation range, although considerable disagreement is recognized in the I_i dependence of $\partial W/\partial I_2$. Also, the fitted parameter values in the E−V slip−link model are fairly well explained using the molecular considerations based on the structural characteristics of the network sample employed here.

Introduction

A large number of theoretical models have been proposed to describe quantitatively the rubber elasticity of cross-linked amorphous polymer networks (elastomers) on the basis of their specific molecular interpretations.[1,2] The presence of chain entanglements (trapped entanglements) arising from the uncrossability of network chains has been considered as a major origin of the significant deviation in the mechanical behavior of real elastomers from the predictions of classical rubber elasticity theories.[1,2] The classical theories are based on the unrealistic assumption of "phantom chains" that the chains do not interact with their environments along their contours.[1,2] Many theoretical attempts have been made to interpret the role of entanglements on rubber elasticity and to model the entanglement effects. These molecular entanglement models for rubber elasticity can be roughly classified into four types of approach: slip−link/hoop models in which trapped entanglements are assumed as "slip−links" moving along network chains[3,4] or as "hoops" through which each network chain threads its way;[5] tube/primitive-path models in which each network chain is confined within "tube"[6−10] or "primitive path"[11,12] formed by the topological constraints of trapped entanglements; fluctuation−constraint models[13−15] in which trapped entanglements act as a constraint on the thermal fluctuation of network chains; network theories based on topological invariants[16,17] in which the topology of entangled polymer systems is rigorously classified and described in terms of topological invariants. The details of each model are referred to the original papers.

So far uniaxial deformation has often been employed to verify the predictive ability of theoretical models in the stress−strain behavior of real elastomers because there exists a lot of experimental data due to the experimental simplicity. However, uniaxial deformation is not sensitive enough to distinguish unambiguously the difference between the models,[18−20] because uniaxial deformation is only a particular one among all the accessible deformations. General biaxial deformation varying independently each of two principal strains (general biaxial strains) is a strict experimental test to identify the models which account for the entanglement effects most successfully and correctly, because the general biaxial strains cover all accessible pure homogeneous deformations for an incompressible material.[1,21] About 15 years ago Gottlieb et al.[22] undertook to compare the predictions of eight molecular models with the biaxial stress−strain data of some cross-linked natural rubbers. They concluded that the three of the eight molecular models tested were relatively successful in accounting for large portions of the experimental data.[22] However, further experimental tests of the molecular theories are needed, because the molecular theories of rubber elasticity have progressed much in the last 10 years. Also, experimental data of a well-characterized network exposed to general biaxial deformations are essential to test rigorously the molecular

* To whom correspondence should be addressed. E-mail: urayama@scl.kyoto-u.ac.jp.

10.1021/ma002166q CCC: $20.00
Published on Web 10/12/2001

models, because the predictions of molecular models contain several parameters related to network structure.

End-linked networks, prepared by end-linking precursor polymer chains, have often been employed as a well-characterized network in the experimental studies aiming at molecular interpretation of rubber elasticity.[23−27] In principle, the end-linking method is capable of controlling the distance between adjacent chemical cross-links as well as the functionality of the cross-link by the length of precursor chain and the functionality of cross-linker, respectively. Also, with the aid of a nonlinear polymerization model for an end-linking system,[28] one can estimate some parameters of network structure (such as the number of network chains and cross-links) from the compositions of initial reactant mixtures and the fraction of unreacted reactants. This is an advantage of end-linked network system for testing unambiguously the molecular theories, because the parameters regarding network structure in molecular theories can be evaluated by the method independent of mechanical testings. On the other hand, in the case of randomly crosslinked networks, there exists no corresponding reliable method to estimate the structural parameters. Therefore, in the experimental tests of molecular theories using randomly crosslinked networks,[18−20,22] the structural parameters have often been treated as fitting parameters, or substituted by hypothetical values, which makes the assessments ambiguous.

Recently, we have carried out the general biaxial deformation experiment for end-linked poly(dimethylsiloxane) (PDMS) networks.[29] The meshes of the PDMS networks used are mainly governed by trapped entanglements because the molecular mass of the precursor linear PDMS is much higher than the critical molecular mass to form entanglement couplings in the un-cross-linked state. The "entanglement-dominated" PDMS network is appropriate to test the molecular theories employing different treatments for entanglement effects. In the present paper, we assess the predictive abilities of five entanglement models (the Edwards−Vilgis slip−link model,[4] several versions of the tube model,[8−10] and the Kloczkowski−Mark−Erman diffused-constraint model[15]) for the general biaxial deformation data of the end-linked PDMS network. It should be noted that none of the theories examined here were treated in the paper of Gottlieb et al.,[22] and in addition, most of them have not yet been experimentally tested using general biaxial deformation data. We exclude here purely phenomenological models as well as those whose underlying physical basis appears to us to be unreasonable. Also we do not include here the Edwards primitive path model[11] and the Marrucci tube model[7] predicting $\partial W/\partial I_2 = 0$, which disagrees with the undoubted experimental evidences[1,29−31] of $\partial W/\partial I_2 \neq 0$ where W is the elastic free energy and I_2 the second invariant of deformation tensor.[22] The details of this point is mentioned in the later section. The Higgs−Ball hoop model,[5] the Graessley primitive path model,[12] and the network theories based on topological invariants[17] are also not examined here because they demand excessibly complicated mathematical formulation for general biaxial deformations[5,12] or they do not provide analytical stress−strain relations because of their extreme algebraic complexity.[17]

Brief Summary of Tested Molecular Theories

Kloczkowski—Mark—Erman Diffused-Constraint Model.[15] The diffused constraint model[15] is the newest version of a series of the fluctuation−constraint models (the constraint−junction model[13] and the subsequent constraint−chain model[14]) which have been developed by Erman et al. The elastic free energy of the fluctuation−constraint models is composed of two terms: One is the contribution of a phantom network, and the other is due to the effects of constraints on fluctuations. The constrained-junction and -chain models allow the constraints to affect the fluctuations of the chemical cross-links or the centers of mass of network chains, respectively. The diffused-constraint model treats the constraints applying continuously along the chains which are more realistic relative to those in the earlier two models. It should be emphasized that the treatments of topological constraints (trapped entanglements) in all the fluctuation−constraint models are fundamentally different from those of the tube models and the slip−link models. In the latter models, the trapped entanglements are explicitly assumed as "physical" (additional) cross-links acting similarly to chemical cross-links on equilibrium elastic modulus. The fluctuation−constraint models consider that the constraints solely depress the fluctuations related to the network chains and cross-links. Accordingly, the fluctuation−constraint models tend to predict definitely lower elastic modulus relative to the tube models and the slip−link models.

The diffused-constraint models assuming the uniform distribution of external constraints along the chain ($w(\theta) = 1$) have the four parameters, the number density of elastic network chains ν, the cycle rank $\xi(= \nu - \mu$; $\mu =$ the number of cross-links), the effective functionality at cross-links f_e, and the measure of constraint k_F. The inverse of k_F is related to the magnitude of thermal fluctuation at cross-links.[15]

Tube Models of Gaylord—Douglas,[8] Kaliske—Heinrich,[9] and Rubinstein—Panyukov.[10] The tube models consider that each network strand is confined within a configurational tube with a harmonic potential modeling topological constraints of entanglements. Several versions of the tube models[6−10] have been reported, and the elastic free energy of the tube models is given by the sum of two terms: One has the Gaussian form due to chain connectivity. The other represents the loss of the degrees of freedom of the chain segments due to their spatial localization originating from entanglements.

The three versions of the tube models employ different assumptions for the dependence of tube dimension on macroscopic deformation. The following power law is used to express the macroscopic deformation dependence of tube diameter:

$$d_i = d_o \lambda_i^{\beta\gamma} \ (i = x, y, z) \tag{1}$$

where d_i and d_o are the tube diameters in the i-direction in the deformed and undeformed states, respectively. The exponent β correlates macroscopic principal ratio λ_i with microscopic one $\lambda_{mic,i}$ as $\lambda_{mic,i} = \lambda_i^{\beta}$ ($0 \leq \beta \leq 1$). The tube models[6−8,10] other than the version of Kaliske et al.[9] assume the affine microscopic deformation for the dimension of network chains, i.e., $\beta = 1$. Kaliske et al.[9] allowed β to vary from zero to unity depending on system in order to consider the nonaffine microscopic deformation due to constraint release effects and/or the

global rearrangements of cross-link upon deformation. The exponent γ represents the dependence of tube diameter on λ_{mic}. Edwards[6] assumed the affine deformation of tube ($\gamma = 1$) in his pioneering work of tube model. The assumption of $\beta = \gamma = 1$ yields the familiar phenomenological Mooney−Rivlin equation, whose poor reproducibility for general deformation behavior has been clearly demonstrated in our preceding paper.[29] Accordingly we do not test here the Edwards tube model. Gaylord et al.[8] employed $\gamma = -1/2$ assuming the constancy of tube volume under deformation. Kaliske et al.[9] and Rubinstein et al.[10] independently derived $\gamma = 1/2$ for slightly or moderately cross-linked networks.

The Gaylord−Douglas and Rubinstein−Panyukov tube models contain two unknown parameters, the contributions of chemical cross-links (G_c) and trapped entanglements (G_e) to equilibrium modulus. The Kaliske−Heinrich tube model has more two parameters, β and δ, in addition to G_c and G_e: δ is a measure of the inextensibility of network chains based on the primitive path concept.

Edwards—Vilgis Slip—Link Model.[4] The slip−link concept represents trapped entanglements as a number N_s of fictitious mobile slip−links which attach two entangled chains. Ball et al.[3] first calculated rigorously the additional elastic free energy due to the presence of slip−links by the replica method. Subsequently Edwards and Vilgis[4] simplified the calculation of the additional free energy and also newly introduced the effect of finite extensibility of network chains on the basis of the primitive path concept. The elastic free energy of the slip−link models consist of the two contributions originating from the presence of chemical cross-links and the slip−links (trapped entanglements). The Edwards−Vilgis slip−link model contains unknown four parameters each of which is related to the characteristics of network topology and slip−links: N_c ($= \nu$) the number of elastic network chains, N_s the number of slip−links, η the measure of slippage of slip−link, and α the inverse of ultimate extensibility of network. The theoretical calculation using the replica method[3] yielded the fixed value $\eta = 0.2343$, but this cannot be true for a real situation in a network.[4] The quantity η in cross-linked networks is treated as a parameter depending on the system, especially the number density of entanglements.[4,32]

Testing Procedure

We test the predictive abilities of the theoretical models for the strain dependence of stress using the *reduced stress*, i.e., the stress divided by equilibrium (small-strain) shear modulus G_o. The use of the reduced stress allows us to restrict our attention to only the strain-dependent predictions as well as to circumvent the difference of each model in the treatments regarding the contributions of trapped entanglements to equilibrium modulus. The latter issue is separately discussed on the basis of the magnitude of G_o.

We assess the strain-dependent predictions simultaneously from two different viewpoints, i.e., the reduced stress−strain relations, and the Rivlin−Saunders method[30] using the invariants of deformation tensor as the variables. The necessity of the simultaneous assessments in the two different ways, and the details of each assessment are described below.

Theoretical Stress. The general stress−strain behavior of a homogeneous, isotropic and elastic material is obtained in terms of the changes in Helmholz free energy (strain energy density function) W together with the three principal ratios λ_1, λ_2, and λ_3 along a set of orthogonal axes. For the biaxial stretching of λ_1 and λ_2 (with $\sigma_3 = 0$), the theoretical nominal stress (the force per unit area of undeformed state) in the ith direction (σ_i) reduced by G_o are calculated from W of each model using the following "Treloar relations":[1,2]

$$\sigma_i/G_o = \frac{2}{V\lambda_i}\left[\frac{\lambda_i^2}{G_o}\left(\frac{\partial W}{\partial \lambda_i^2}\right) - \frac{\lambda_3^2}{G_o}\left(\frac{\partial W}{\partial \lambda_3^2}\right)\right]_{T,V} \quad (2a)$$

$$= \frac{2}{V\lambda_i}\left[\frac{\lambda_i}{G_o}\left(\frac{\partial W}{\partial \lambda_i}\right) - \frac{\lambda_3}{G_o}\left(\frac{\partial W}{\partial \lambda_3}\right)\right]_{T,V} \quad (2b)$$

where V is the volume of network. The relation $\lambda_3 = 1/(\lambda_1\lambda_2)$ holds due to the incompressibility of the rubbery network. The expressions of $\partial W/\partial \lambda_i^2$ or $\partial W/\partial \lambda_i$ for each model are given in Table 1.

Rivlin—Saunders Method.[30] The function W is customarily expressed as a function of the three invariants I_1, I_2, I_3 of Green's deformation tensor. The third invariant $I_3 = \lambda_1^2\lambda_2^2\lambda_3^2$ equals one for an incompressible material. The PDMS network used in the present study is reasonably well assumed to be incompressible.[29] As the result, W can be expressed as a function of the two invariants I_1, I_2:

$$W = W(I_1, I_2) \quad (3)$$

where

$$I_1 = \lambda_1^2 + \lambda_2^2 + \lambda_3^2 \quad (4a)$$

$$I_2 = \lambda_1^2\lambda_2^2 + \lambda_2^2\lambda_3^2 + \lambda_3^2\lambda_1^2 \quad (4b)$$

The reduced biaxial stress−strain relation, i.e., $\sigma_i/G_o - \lambda_j$ ($i,j = 1,2$) relation, is related to the derivatives of W with respect to I_1 and I_2 (reduced by G_o) as follows.[1,30]

$$\frac{1}{G_o}\frac{\partial W}{\partial I_1} = \frac{1}{2(\lambda_1^2 - \lambda_2^2)}\left[\frac{\lambda_1^3\sigma_1/G_o}{\lambda_1^2 - (\lambda_1\lambda_2)^{-2}} - \frac{\lambda_2^3\sigma_2/G_o}{\lambda_2^2 - (\lambda_1\lambda_2)^{-2}}\right] \quad (5a)$$

$$\frac{1}{G_o}\frac{\partial W}{\partial I_2} = \frac{-1}{2(\lambda_1^2 - \lambda_2^2)}\left[\frac{\lambda_1\sigma_1/G_o}{\lambda_1^2 - (\lambda_1\lambda_2)^{-2}} - \frac{\lambda_2\sigma_2/G_o}{\lambda_2^2 - (\lambda_1\lambda_2)^{-2}}\right] \quad (5b)$$

Using eqs 4 and 5, $\partial W/\partial I_1$ and $\partial W/\partial I_2$ as a function of I_1 and I_2 are obtained from the biaxial stress−strain relation. The analysis of W using the Rivlin−Saunders method has often been used in phenomenological studies,[1,29−31] but this analysis is also significant from the viewpoint of molecular theories. Rivlin and Saunders[30] first pointed out that $\partial W/\partial I_2$ for a real elastomer was finite, contrary to the postulate of the classical rubber elasticity theories ($\partial W/\partial I_2 = 0$ from $W = C(I_1 - 3)$), using eqs 4 and 5 in their pioneering biaxial elongation experiment of a cross-linked natural rubber. As Gottlieb et al.[22] suggested, it is necessary to test the strain-dependent predictions by both of the two different ways, i.e., the λ_i dependence of σ_j ($i,j = 1,2$) and the I_i dependence of $\partial W/\partial I_j$ ($i,j = 1,2$). Even if a theoretical model is successful in reproducing the experimental $\sigma - \lambda$ relation, it is not guaranteed that the model is also successful for the I_i dependence of $\partial W/\partial I_j$, and vice

Table 1. Theoretical Expressions for the Tested Models

model	G_0	$\partial W/\partial\lambda$ or $\partial W/\partial\lambda^2$	fitted parameter
		Diffused-Constraint Model	
Kloczkowski–Mark–Erman	$\xi RT\left(1+\frac{\nu}{\xi}\int_0^1 w(\theta)\frac{1+\kappa(\theta)}{(1+\kappa(\theta))^4}\kappa(\theta)^2 d\theta\right)$, $\kappa(\theta)=\kappa_F\left[1+\frac{(f_e-2)^2\theta(1-\theta)}{f_e-1}\right]$	$\frac{\partial W}{\partial\lambda^2}=\frac{1}{2}\xi RT\left(1+\frac{\nu}{\xi}\int_0^1 w(\theta)\left(\frac{B_i(\theta)\dot{B}_i(\theta)}{B_i(\theta)+1}+\frac{D_i(\theta)\dot{D}_i(\theta)}{D_i(\theta)+1}\right)d\theta\right)$, $B_i(\theta)=\frac{\kappa(\theta)^2(\lambda_i^2-1)}{(\lambda_i^2+\kappa(\theta))^2}$, $D_i(\theta)=\frac{B_i(\theta)\lambda_i^2}{\kappa(\theta)}$, $\dot{B}_i(\theta)=\frac{\partial B_i(\theta)}{\partial\lambda_i^2}$, $\dot{D}_i(\theta)=\frac{\partial D_i(\theta)}{\partial\lambda_i^2}$	κ_F
		Tube Model	
Gaylord–Douglas	$G_c+\frac{1}{2}G_{loc}$ ($G_{loc}=A(\nu RT)+G_N^0$)	$\frac{\partial W}{\partial\lambda_i}=G_c\lambda_i+G_{loc}$	G_{loc}/G_c
Kaliske–Heinrich	$G_c(1-2\delta^2)+\beta^2 G_e^*$ ($G_e^*=C\cdot G_N^0$)	$\frac{\partial W}{\partial\lambda_i}=G_c\lambda_i\left(\frac{1-\delta^2}{(1-\delta^2(\sum_{j=1}^3\lambda_j-3))^2}-\frac{\delta^2}{1-\delta^2(\sum_{j=1}^3\lambda_j-3)}\right)-2\beta G_e^*\lambda_i^{-\beta-1}$	G_e^*/G_c, β, δ
Rubinstein–Panyukhov	G_c+G_e	$\frac{\partial W}{\partial\lambda_i}=G_c\lambda_i+G_e\left(1+\frac{1}{\lambda_i^2}\right)$	G_e/G_c
		Slip–Link Model	
Edwards–Vilgis	$N_cRT\frac{1-2\alpha^2+O(\alpha^4)}{(1-3\alpha^2)^2}+N_sRT\frac{1-2\alpha^2+2\alpha^2\eta+2\alpha^2\eta^2+O(\alpha^4)}{(1+\eta)^2(1-3\alpha^2)^2}$	$\frac{\partial W}{\partial\lambda_i^2}=Kc_i+Ks_i$, $A=1-\alpha^2\sum_{j=1}^3\lambda_j^2$, $Kc_i=\frac{1}{2}N_cRT\frac{1}{A^2}(1-2\alpha^2+\alpha^4\sum_{j=1}^3\lambda_j)$, $Ks_i=\frac{1}{2}N_sRT\left(\frac{(1+\eta)(1-\alpha^2)}{A(1+\eta\lambda_i^2)^2}+\frac{\eta}{1+\eta\lambda_i^2}-\frac{\alpha^2}{A}+\sum_{j=1}^3\frac{(1+\eta)(1-\alpha^2)\alpha^2\lambda_j^2}{A^2(1+\eta\lambda_j^2)}\right)$	N_s/N_c, η, α

Table 2. Characteristics of End-Linked PDMS Network

polymer concn (wt %)	$M_{n,p}$ (g/mol)	r	w_{sol}[a] (wt %)	G_o[b] (Pa)	ν[c] (mol/m^3)	μ[c] (mol/m^3)	f_e[c]	$M_{n,el}$[c] (g/mol)
70	4.66×10^4	1.3	7.50	6.49×10^4	3.22	2.04	3.16	8.25×10^4

[a] For reactants excluding unreactive diluent. [b] From biaxial elongation experiment.[29] [c] From the Miller–Macosko model[28] for nonlinear polymerization.

versa. Therefore, we test the strain-dependent predictions of each model from these two viewpoints, and we evaluate the fitting parameters in each model so that they can reproduce most satisfactorily the experimental data simultaneously in both the "stress-strain" and the "$I_i - \partial W/\partial I_j$" plots.

Equilibrium Modulus. The molecular theories have different expressions for G_o depending on their considerations for entanglement effects. The expressions for G_o of each model are listed in Table 1. Each theoretical modulus contains the parameters related to network topology and those peculiar to the model. The former parameters (such as ν, ξ) are estimated from a nonlinear polymerization model[28] with some data about the reaction conditions. The latter parameters are evaluated from the best fitting procedure for the strain-dependent predictions.

Characteristics of the End-Linked Network Sample

Multiaxial Deformation Experiments. The quasi-equilibrium stress–strain relationships of uniaxial, biaxial elongation and uniaxial compression were obtained at 40 °C. The experimental details are referred to the preceding paper.[29]

Structural Parameters. In the present analysis, we employed the experimental results of the end-linked PDMS network prepared from 70 wt % solution, instead of that from melt, because a larger deformation range was investigated for the solution-endlinked network due to its higher extensibility.[29] It is to be noted that the network prepared from 70 wt % solution possesses elastically "entanglement-dominated" character as in the case of the melt-endlinked one, since the elastic behavior of both the networks is governed by a common type of phenomenological strain energy density function,[29] and the concentration dependence of equilibrium modulus is nearly square.[29]

The PDMS network was prepared by end-linking linear precursor PDMS with tetrafunctional cross-linker in the presence of 30 wt % nonvolatile diluent. The number-average molecular mass of the precursor PDMS ($M_{n,p}$), the molar ratio of functional groups in the precursor PDMS to those in the cross-linker (r), and the weight fraction of unreacted (soluble) reactants (w_{sol}) are given in Table 2. The details of the sample preparation were described in the foregoing paper.[29] After the end-linking reaction, the sample sheet was used for the measurements without removing the nonvolatile diluent.

Each molecular theory contains the parameters related to network structure. The parameters such as ν and ξ are estimated from the compositions of initial reactant mixture and the data of w_{sol} on the basis of the Miller–Macosko model for nonlinear polymerization.[28] The estimated values of ν, μ, ξ, and f_e are shown in Table 2. The number-average molecular mass of elastic chains (excluding any attached dangling chains)

$M_{n,el}$ estimated is also included in Table 2. The larger value of $M_{n,el}$ relative to $M_{n,p}$ is due to a finite amount of w_{sol} as well as the use of $r > 1$ (resulting from the optimization of reaction condition).[25,29] The ratio of the entanglement spacing (M_e) to $M_{n,el}$ is fairly large (ca. 6), which verifies the entanglement-dominated character of the network used here. The value of M_e was estimated to be 1.3×10^4 g/mol by considering the dilution effect of entanglements[33] as $M_e = M_{e,melt} \times \phi^{-1}$ with $M_{e,melt} = 8.1 \times 10^3$ g/mol[33] and $\phi = 0.625$ where ϕ is the effective polymer fraction considering w_{sol}.

In the cases of the slip−link model[4] and the tube models,[8−10] the elastic contribution of trapped entanglements relative to that of chemical cross-links G_e/G_c ($\approx N_s/N_c$) is an important parameter in testing the strain-dependent predictions. The ratio G_e/G_c is related to ν, ξ, and G_o as described below. We evaluate the admissible range of G_e/G_c for the network sample used here in order to avoid the fictitious success with an unrealistic fitted value of G_e/G_c in the tests of strain-dependent predictions. The equilibrium modulus of the slip−link model and the tube models is given by the sum of G_c and G_e:

$$G_o = G_c + G_e = (\nu - h\mu)\,RT + G_e \qquad (6)$$

where G_c is between the modulus of phantom network (ξRT) and that of the affine network (νRT) and h is an empirical parameter varying from zero to unity, depending on the degree of thermal fluctuation of cross-links. The entanglement modulus G_e is correlated with the quasi-plateau shear modulus of un-cross-linked polymer melt (G_N^o), but the relation of G_e and G_N^o depends on the models as shown in Table 1. Since h and G_e are not determinable independently, the value of G_e/G_c cannot be uniquely determined from ν, μ, and G_o, but it has the following admissible range:

$$(G_o/\nu RT) - 1 \le G_e/G_c \le (G_o/\xi RT) - 1 \qquad (7)$$

Using the values of G_o, ξ, and ν in Table 2, $6.7 \le G_e/G_c \le 20$ is obtained as the accessible range of G_e/G_c for the network sample used here. The minimum and maximum of G_e/G_c correspond to the case of affine ($h = 0$) and phantom modulus ($h = 1$) for G_c, respectively.

Results and Discussion

Kloczkowski—Mark—Erman Diffused-Constraint Model.[15] Figures 1 and 2 show the comparisons of the experimental data with the predictions of the diffused-constraint model for the λ_2 dependences of the reduced stresses σ_1/G_o (Figure 1a) and σ_2/G_o (Figure 1b), and the I_i dependence of the reduced derivatives $(\partial W/\partial I_j)/G_o$ ($i,j = 1,2$) (Figure 2). The inset in Figure 1b illustrates the comparisons for uniaxial compression. The subscripts 1 and 2 in σ and λ represent the principal axes of larger and smaller strains, respectively. In Figure 1, the theoretical predictions are represented by solid lines, and each line stands for the reduced stresses at same λ_1. The values of ν, ξ, and f_e in Table 2, and $w(\theta) = 1$ were used in the calculations of the theoretical stresses. One adjustable parameter k_F was employed in data fitting, and the best fit procedure yielded $k_F = 2.9$. The predictions are relatively successful in reproducing the λ_2 dependence of the reduced stresses, though the theory underestimates both the reduced principal stresses at the large deformations of $\lambda > 1.7$. The predictions fit successfully the data of $(\partial W/\partial I_2)/G_o$, while almost no dependence of the theoretical $(\partial W/\partial I_1)/G_o$ on I_i is not in accord with the experimental results.

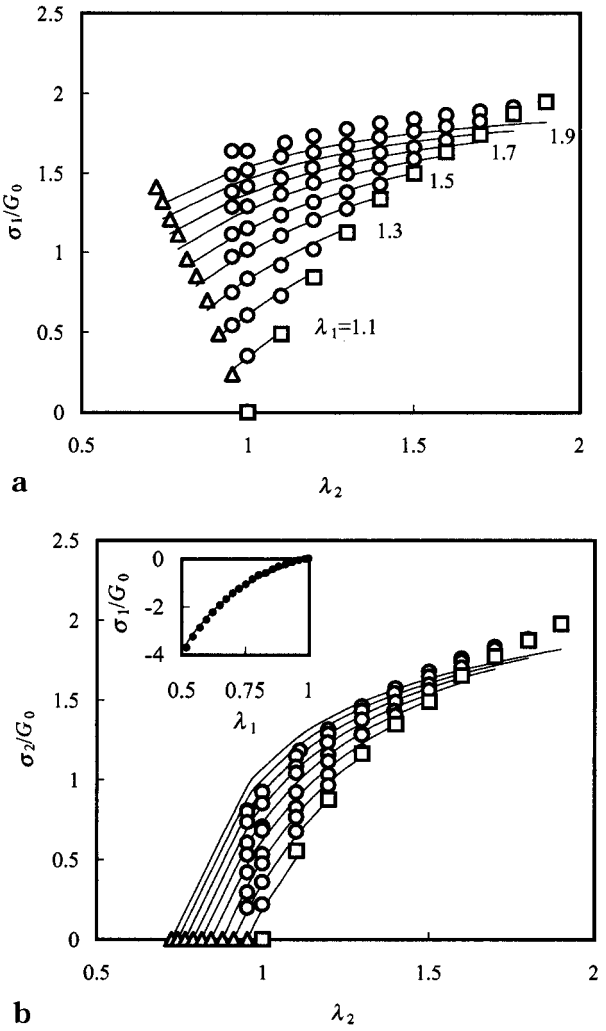

Figure 1. Comparisons of the experimental λ_2 dependence of reduced principal stresses (a) σ_1/G_o and (b) σ_2/G_o with the best-fitted predictions of the diffused-constraint model with $\kappa_F = 2.9$ (solid lines). Each line stands for the theoretical reduced stresses at same λ_1. The triangle and rectangular symbols correspond to uniaxial and equibiaxial elongation, respectively. The inset of Figure 1b shows the comparisons for uniaxial compression. The values of ν, ξ, and f_e in Table 2 and $w(\theta) = 1$ were employed in the calculations of the theoretical curves.

The parameter κ_F is considered to be a measure of the severity of entanglement constraint on the thermal fluctuation of cross-links.[15] The range of κ_F can vary from zero (phantom) to infinity (affine). The parameter κ_F (and the similar parameters κ and κ_G in the constraint−junction[13] and constraint−chain models,[14] respectively) has been used as a semiempirical parameter in data fitting procedure.[13−15] At present, there exists no molecular approach estimating the magnitude of κ_F independently of mechanical testings, which precludes the detailed discussion about the validity of $\kappa_F = 2.9$.

It is very important to point out that the diffused-constraint model gives too small a value of G_o ($G_o = 5.22 \times 10^3$ Pa) relative to the experimental value ($G_o = 6.49 \times 10^4$ Pa). The theoretical value of G_o, calculated using ν and ξ in Table 2 and $k_F = 2.9$, is 1 order of magnitude smaller than the experimental one. This marked underestimation of G_o is due to the fact that

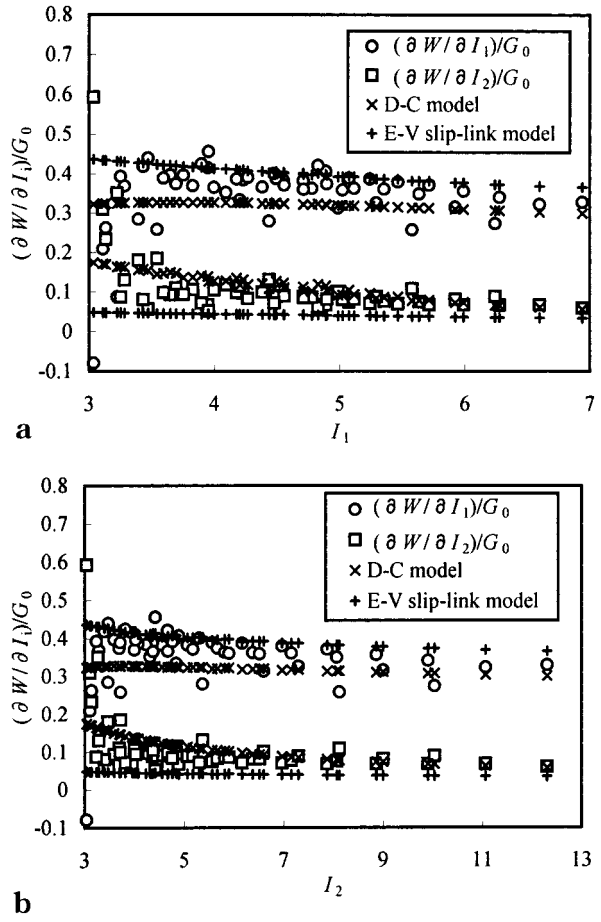

Figure 2. Comparisons of the experimental reduced derivatives $(\partial W/\partial I_i)/G_o$ (i = 1,2) as a function of (a) I_1 and (b) I_2 with the best-fitted predictions of the diffused-constraint model and the Edwards−Vilgis slip−link model. The parameter values used are the same as those for the reduced stresses.

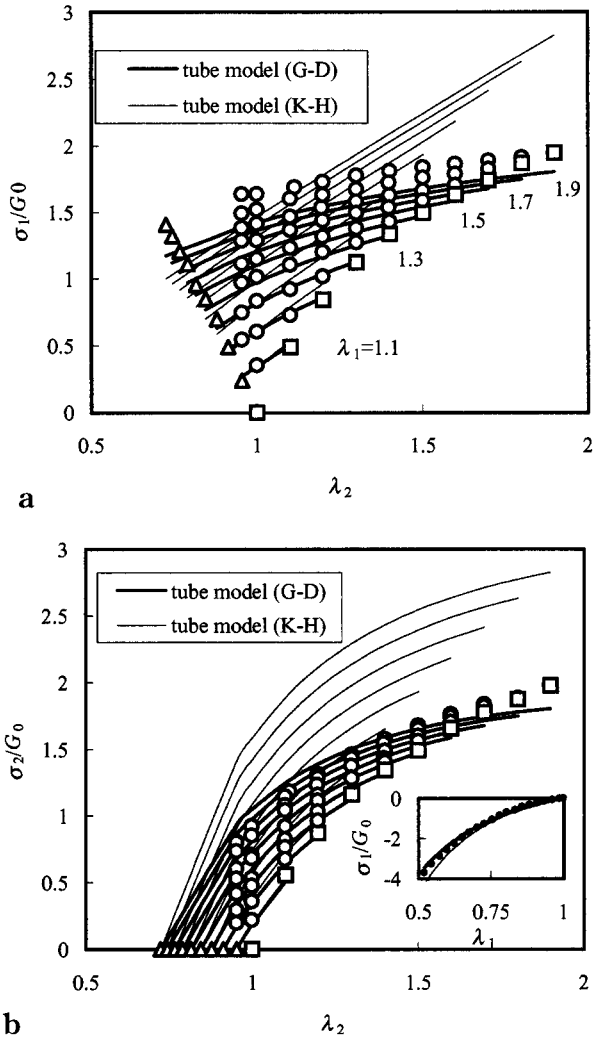

Figure 3. Comparisons of the experimental λ_2 dependence of reduced principal stresses (a) σ_1/G_o and (b) σ_2/G_o with the best-fitted predictions of the Gaylord−Douglas tube model with $G_{loc}/G_c = 13.4$ (bold solid lines) and the Kaliske−Heinrich tube model with $G_e^*/G_c = 9.3$, $\beta = 0.85$, and $\delta = 0$ (solid lines). Each line stands for the theoretical reduced stresses at same λ_1. The triangle and rectangular symbols correspond to uniaxial and equibiaxial elongation, respectively. The inset of part b shows the comparisons for uniaxial compression.

the diffused-constraint model does not consider trapped entanglements as the additional cross-links contributing to equilibrium modulus (in contrast to the tube models and the slip−link models). Actually, the upper limit of G_o in the diffused-constraint model for tetrafunctional network is only 1.5 times of affine modulus (νRT).[15] Since the experimental value of G_o for the sample used here is much larger than $1.5\nu RT$, the underestimation of G_o by the diffused-constraint model is inevitable. It is noticed that the entanglement-dominated character of the network used here, in which ν is much smaller relative to the number density of trapped entanglements, clearly reveals the limit of the prediction of the diffused-constraint model for G_o. Due to the substantial underestimation of G_o, the relatively successful data-fit of the strain-dependent predictions using "reduced" stresses (in which the effect of G_o is eliminated) must be treated with extreme caution. The same caution should be applicable to the earlier versions of constraint−fluctuation theories such as constraint−junction[13] and constraint−chain models[14] using essentially the same treatments of trapped entanglements.

Tube Models of Gaylord—Douglas,[8] Kaliske—Heinrich,[9] and Rubinstein—Panyukov.[10] Figures 3 and 4 show the results of the fitting procedures for the strain-dependent predictions of the tube models of Gaylord−Douglas (G−D) and Kaliske−Heinrich (K−H). For the G−D model, one adjustable parameter G_{loc}/G_c was employed in the fitting procedure. According to their definition,[8] the one-half of the front factor G_{loc} of the topological constraint term in W corresponds to G_e in eq 7, which yields $6.7 \le (1/2)G_{loc}/G_c \le 20$ as the accessible range of G_{loc}/G_c. The best-fit results for the G−D model were obtained when G_{loc}/G_c =13.4. It can be seen in Figure 3 that the G−D model is successful up to the middle range of deformations, but the model definitely underestimates σ_1/G_o and σ_2/G_o in the large deformation region of $\lambda_i > 1.6$. It is found in Figure 4 that the G−D model is relatively successful in reproducing the behaviors of both the reduced derivatives.

The value of G_{loc} is estimated to be $G_{loc} = 1.1 \times 10^5$ Pa using $G_c = \nu RT$ (because the fitted value of G_{loc}/G_c is the minimum in eq 7). The G−D model considers that G_{loc} depends on both the network connectivity and the plateau modulus of the un-cross-linked melt as $G_{loc} = A(\nu RT) + G_N^o$ where A is an unspecified constant.[8] The employment of $G_N = G_N^o\phi^2$ with the effective polymer concentration[33] ($\phi = 0.625$) and $G_N^o = 2.0 \times 10^5$ Pa[34] yields $A = 4.1$. However, the ambiguity of the original definition[8] of A prevents a detailed discussion about the absolute value of A.

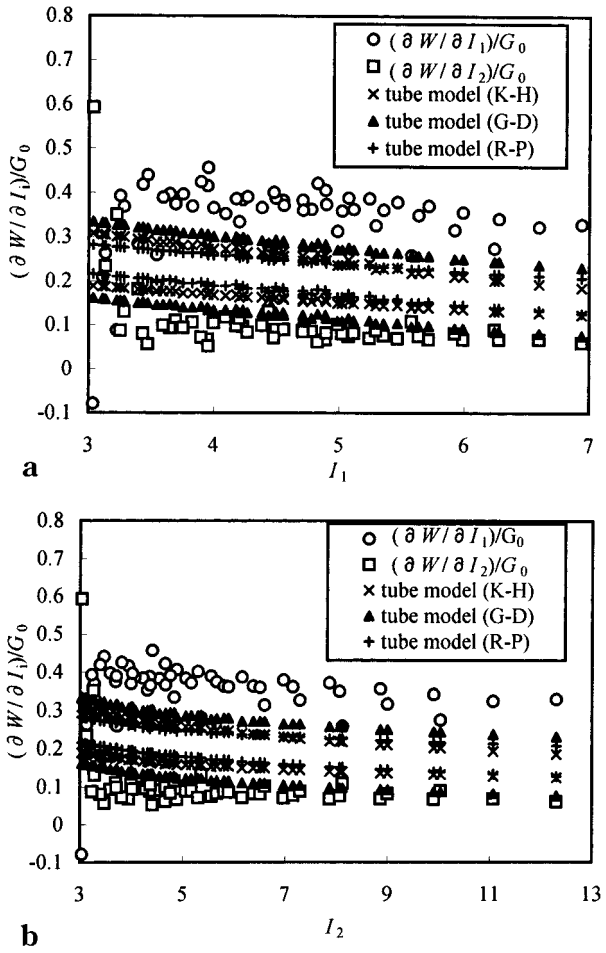

Figure 4. Comparisons of the experimental reduced derivatives $(\partial W/\partial I_i)/G_o$ (i = 1,2) as a function of (a) I_1 and (b) I_2 with the best-fitted predictions of the tube models of Gaylord−Douglas, Kaliske−Heinrich and Rubinstein−Panyukov versions. The parameter values used are the same as those for the reduced stresses.

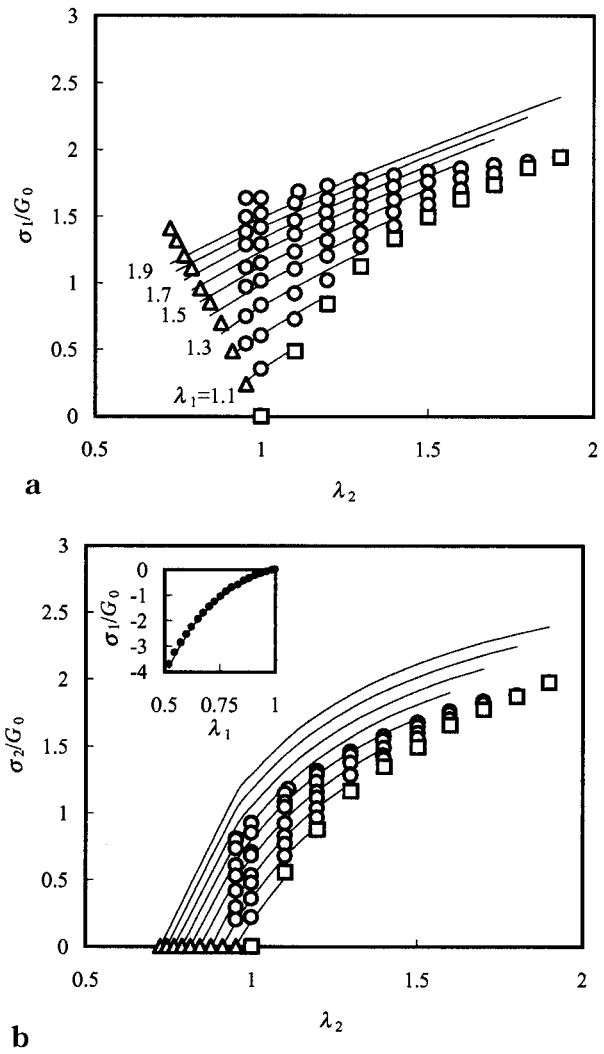

Figure 5. Comparisons of the experimental λ_2 dependence of reduced principal stresses (a) σ_1/G_o and (b) σ_2/G_o with the best-fitted predictions of the Rubinstein−Panyukov tube model with G_e/G_c = 6.7 (solid lines). Each line stands for the theoretical reduced stresses at same λ_1. The triangle and rectangular symbols correspond to uniaxial and equibiaxial elongation, respectively. The inset of part b shows the comparisons for uniaxial compression.

For the K−H model, three adjustable parameters G_e^*/G_c, β ($0 \le \beta \le 1$), δ ($\delta \ge 0$) were employed in the fitting procedures. The relation of G_e^* and G_e in eq 7 in the K−H models is given by $G_e = \beta^2 G_e^*$ where G_e^* is a modulus proportional to G_N^o ($G_e^* = CG_N^o$ where C is the system-dependent constant).[9] The accessible range of G_e/G_c in eq 7 gives $6.7 \le \beta^2 G_e^*/[G_c(1 - 2\delta^2)] \le 20$. The best fit procedure with adjustable ranges of $\beta^2 G_e^*/[G_c(1 - 2\delta^2)]$, $0 \le \beta \le 1$, and $\delta \ge 0$ yielded G_e^*/G_c = 9.3, β = 0.85, and δ = 0. It can be seen, however, that the quality of the fit is poor, and the predicted strong λ_2 dependence of σ_1/G_o is far from the real behavior. In addition, the model obviously overestimates σ_2/G_o over a wide range of deformations. The employment of a finite value of δ yields the upturn of the stress−strain curve at high elongation, which does not improve the quality of the data fit.

Figures 4 and 5 illustrate the results of the experimental tests for the strain-dependent predictions of the Rubinstein−Panyukov (R−P) tube model. One adjustable parameter G_e/G_c with the admissible range of eq 7 was used for data fittings. Poor reproducibility of the R−P model for the experimental results is evident in both the figures, especially for both the reduced principal stresses. The predictions of the R−P and K−H models for the reduced derivatives are almost indistinguishable.

None of the three versions of tube models consistently reproduce in successful level the experimental reduced stress−strain data. Among the three versions of tube model tested here, the G−D model is the most successful in reproducing the data, but the quality of data fit is not satisfactory.

Edwards—Vilgis Slip—Link Model.[4] The comparisons of the experimental data with the strain-dependent predictions of the Edwards−Vilgis (E−V) slip−link model are illustrated in Figures 2 and 6. Three adjustable parameters, N_s/N_c, η, and α_s, were used for data fittings. It can be seen that the E−V slip−link model with N_s/N_c = 7.0, η = 0.08, and α = 0.15 satisfactorily reproduces the λ_2 dependence of both the reduced principal stresses over a wide deformation range, although the prediction slightly underestimates σ_2/G_o at large deformations of $\lambda_1 > 1.6$. The prediction for $(\partial W/\partial I_1)/G_o$ is also in good agreement with the experimental data. However, the almost zero dependence of the theoretical $(\partial W/\partial I_2)/G_o$ on I_i disagrees with the finite dependence observed experimentally.

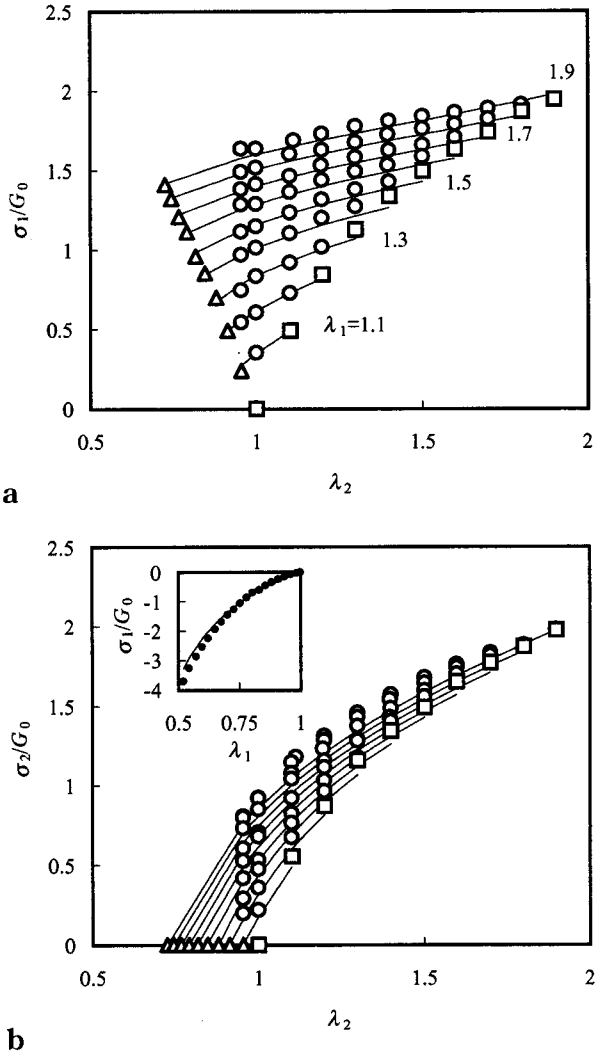

Figure 6. Comparisons of the experimental λ_2 dependence of reduced principal stresses (a) σ_1/G_o and (b) σ_2/G_o with the best-fitted predictions of the Edwards−Vilgis slip−link model with $N_s/N_c = 7.0$, $\eta = 0.08$, and $\alpha = 0.15$ (solid lines). Each line stands for the theoretical reduced stresses at same λ_1. The triangle and rectangular symbols correspond to uniaxial and equibiaxial elongation, respectively. The inset of part b shows the comparisons for uniaxial compression.

The parameter η is a measure for the amount of sliding of one entanglement between two consecutive cross-links. Vilgis et al.[32] roughly related η to the topological characters of networks as $\eta = M_e/M_c$ where M_c and M_e are the molecular mass between cross-links and that between entanglements, respectively. Using $M_c = M_{n,el}$ and $M_e = 1.3 \times 10^4$ g/mol (see the former section), the value of M_e/M_c is estimated to be 0.16, which is slightly larger than the fitted value of $\eta = 0.08$. However, the agreement may be considered satisfactory in view of the wide accessible range of η ($0 < \eta < \infty$) as well as the roughness of the estimations used.

The parameter α for entanglement-dominated networks is related to the extensibility of the chains between entanglements as $\alpha = b/a$ where b and a are the Kuhn segment length and the step length of primitive path, i.e., the entanglement distance, respectively.[4] The ratio b/a is correlated with G_N^o on the basis of the Doi−Edwards theory[35] as $b/a = [mG_N^o/(\rho RT)]^{1/2}$ where m and ρ is the molecular mass of repeating unit and the polymer density, respectively. The resulting value of $b/a \approx 0.08$ is smaller than but not so far from the fitted value of $\alpha = 0.15$.

Table 3. Best-Fit Parameter Values

model	parameters	rms[b] × 10^2
	Diffused-Constraint Model	
Kloczkowski−Mark−Erman	$\kappa_F = 2.9$	0.493
	Tube Models	
Gaylord−Douglas	$G_{loc}/G_c = 13.4$[a]	0.704
Kaliske−Heinrich	$G_e^*/G_c = 9.3$,[a] $\beta = 0.85$, $\delta = 0$	3.45
Rubinstein−Panyukov	$G_e/G_c = 6.7$[a]	1.75
	Slip−Link Model	
Edwards−Vilgis	$N_s/N_c = 7.0$,[a] $\eta = 0.08$, $\alpha = 0.15$	0.487

[a] The admissible range of eq 7 was used in the best-fit procedures. [b] The value of rms was calculated by $(1/2n)\{\sum_{i=1}^{2}\sum_n(\sigma_{i,th}/G_o - \sigma_{i,exp}/G_o)^2\}^{1/2}$ where n is the number of experimental data points, and $\sigma_{i,th}$ and $\sigma_{i,exp}$ are the theoretical and experimental values, respectively.

The quantity N_s/N_c is the number ratio of trapped entanglements to elastic network chains, and it approximately corresponds to the relative elastic contribution of the topological constraint term to the term of network connectivity. The fitted value of $N_s/N_c = 7.0$ is within the accessible range of G_e/G_c ($\approx N_s/N_c$) for the network sample used here (eq 7). According to the definition of G_o in Table 1, the fitted parameter values and ν ($=N_c$) in Table 2 yields $G_o = 6.46 \times 10^4$ Pa, which is in good agreement with the experimental value.

Evidently, among the five entanglement models tested here, the E−V slip−link model shows the most successful reproducibility in the two different plots for the strain dependence of stresses as well as the magnitude of G_o, although the disagreement in the I_i dependence of $\partial W/\partial I_2$ is not small. This is also recognized by the result that the E−V slip−link model shows the smallest value of the root of mean square (rms) for the differences in experimental and theoretical reduced stresses. The value of rms for each model is shown in Table 3 together with the best-fitted parameter values used. In addition, the best-fitted values of the two parameters, η and α, in the E−V slip−link model are in relatively good agreement with the estimations based on the structural characteristics of the network used here. A further investigation using end-linked networks with smaller values of $M_{n,el}/M_e$ enables us to discuss the dependence of the model parameters on $M_{n,el}/M_e$, which will lead to a more detailed assessment of the molecular theories. This is a subject for our future work.

Summary

Five molecular models of rubber elasticity employing different treatments of entanglement effects (the Kloczkowski−Mark−Erman diffused-constraint model, the tube models of three different versions, and the Edwards−Vilgis slip−link model) were tested using the biaxial deformation and uniaxial compression data of an end-linked PDMS network. The sample of end-linked PDMS network used here has the "entanglement-dominated" character with the high ratio (ca. 6) of entanglement spacing to the chain length between adjacent cross-links. The parameters related to network structure such as ν and ξ, which are involved in the theoretical predictions, were estimated (independently of mechanical testing) on the basis of a nonlinear

polymerization model for end-linking system using the data for the composition of initial reactants and w_{sol}.

Using the reduced stress (the stress divided by equilibrium shear modulus G_o), the reproducibility of the strain-dependent predictions of each model for the experimental results was investigated from two different viewpoints, i.e., the dependence of the reduced stresses on the principal ratio, and the dependence of $(\partial W/\partial I_i)/G_o$ on I_j $(i,j = 2)$ using the invariants of deformation tensor as the variables (the Rivlin−Saunders method).

The strain-dependent predictions of the diffused-constraint model with $k_F = 2.9$ are in relatively good agreement with the experimental reduced stress − strain data except for large deformation region. It is to be emphasized, however, that the diffused-constraint model definitely underestimates the magnitude of G_o. This is because the diffused-constraint model does not consider trapped entanglements as the additional cross-links contributing to equilibrium modulus, in contrast to the slip−link model and the tube models. Due to the obvious underestimation of G_o, one must treat the relatively successful fit of the diffused constraint model for the reduced stresses with extreme caution.

For the tube models, none of the three versions (the Gaylord−Douglas, Kaliske−Heinrich, or Rubinstein−Panyukov) using different assumptions for the deformation dependence of tube dimension reproduce the experimental data satisfactorily.

The E−V slip−link model fit the experimental data most successfully among the five molecular approaches tested here. The E−V slip−link model satisfactorily reproduces a large portion of the experimental data, though the predicted almost constant $\partial W/\partial I_2$ against I_i is not in accord with the finite dependence observed. Also, the absolute values of the best-fitted parameters ($\eta = 0.08$ and $\alpha = 0.15$) in the model are fairly well explained using the molecular approaches based on the topological characteristics of the network sample used.

Note added in proof. Recently the paper of a "double tube" model for rubber elasticity has appeared.[37] However, attempts to derive the theoretical biaxial stress−strain relation encounter mathematical difficulties.

Acknowledgment. This work is partly supported by a Grant-in-Aid from the Ministry of Education, Science, Sports, and Culture of Japan (Ns. 09750990 and 12875127).

References and Notes

(1) Treloar, L. R. G. *The Physics of Rubber Elasticity*, 3rd ed.; Oxford University Press: Oxford, England, 1975.
(2) Erman, B.; Mark, J. E. *Structure and Properties of Rubberlike Networks*; Oxford University Press: Oxford, England, 1997.
(3) Ball, R. C.; Doi, M.; Edwards, S. F.; Warner, M. *Polymer* **1981**, *22*, 1010.
(4) Edwards, S. F.; Vilgis, T. A. *Polymer* **1986**, *27*, 483; *Rep. Prog. Phys.* **1988**, *51*, 243.
(5) Higgs, P. G.; Ball, R. C. *Europhys. Lett.* **1989**, *8*, 357.
(6) Edwards, S. F. *Proc. Phys. Soc.* **1967**, *92*, 9.
(7) Marrucci, G. *Macromolecules* **1981**, *14*, 434.
(8) Gaylord, R. J.; Douglas, J. F. *Polym. Bull.* **1987**, *18*, 347; **1990**, *23*, 529.
(9) Kaliske, M.; Heinrich, G. *Rubber Chem. Technol.* **1999**, *72*, 602.
(10) Rubinstein, M.; Panyukov, S. *Macromolecules* **1997**, *30*, 8036.
(11) Edwards, S. F. *Br. Polym. J.* **1977**, *9*, 140.
(12) Graessley, W. W. *Adv. Polym. Sci.* **1982**, *46*, 67.
(13) Flory, P. J.; Erman, B. *Macromolecules* **1982**, *15*, 800.
(14) Erman, B.; Monnerie, L. *Macromolecules* **1989**, *22*, 3342.
(15) Kloczkowski, A.; Mark, J. E.; Erman, B. *Macromolecules* **1995**, *28*, 5089.
(16) Deam, R. T.; Edwards, S. F. *Philos. Trans. R. Soc. London, Ser. A* **1976**, *280*, 317.
(17) Iwata, K. *J. Chem. Phys.* **1982**, *76*, 6363; **1985**, *83*, 1969.
(18) Gottlieb, M.; Gaylord, R. J. *Polymer* **1983**, *24*, 1644.
(19) Higgs, P. G.; Gaylord, R. J. *Polymer* **1990**, *31*, 70.
(20) Meissner, B. *Polymer* **2000**, *41*, 7827.
(21) Tschoegl, N. W.; Gurer, C. *Macromolecules* **1985**, *18*, 680.
(22) Gottlieb, M.; Gaylord, R. J. *Macromolecules* **1987**, *20*, 130.
(23) Gottlieb, M.; Macosko, C. W.; Benjamin, K. O.; Mayers, K. O.; Merril, E. W. *Macromolecules* **1981**, *14*, 1039.
(24) Mark, J. E. *Adv. Polym. Sci.* **1982**, *44*, 1.
(25) Patel, S. K.; Malone, C.; Cohen, C.; Gillmor, J. R.; Colby, R. H. *Macromolecules* **1992**, *25*, 5241.
(26) Urayama, K.; Kohjiya, S. *J. Chem. Phys.* **1996**, *104*, 3352; *Eur. Phys. J. B.* **1998**, *2*, 75.
(27) Urayama, K.; Kawamura, T.; Kohjiya, S. *J. Chem. Phys.* **1996**, *105*, 4833.
(28) Miller, D. R.; Macosko, C. W. *Macromolecules* **1976**, *9*, 206.
(29) Kawamura, T.; Urayama, K.; Kohjiya, S. Multiaxial Deformations of End-linked Poly(dimethylsiloxane) Networks: 1. Phenomenological Approach to Strain Energy Density Function. *Macromolecules* **2001**, *34*, 8252.
(30) Rivlin, R. S.; Saunders, D. W. *Philos. Trans. R. Soc.* **1951**, *A243*, 251.
(31) Kawabata, S.; Matsuda, M.; Tei, K.; Kawai, H. *Macromolecules* **1981**, *14*, 154.
(32) Vilgis, T. A.; Erman, B. *Macromolecules* **1993**, *26*, 6657.
(33) Ferry, J. D. *Viscoelastic Properties of Polymers*, 3rd ed.; Wiley: New York, 1980.
(34) Plazek, D. J.; Dannhuser, W.; Ferry, J. D. *J. Colloid Sci.* **1961**, *16*, 101.
(35) Doi, M.; Edwards, S. F. *The Theory of Polymer Dynamics*; Oxford University Press: New York, 1986.
(36) Valles, E. M.; Macosko, C. *Macromolecules* **1979**, *12*, 673.
(37) Mergell, B.; Everaers, R. *Macromolecules* **2001**, *34*, 5675.

MA002166Q